Supplementary information

Ex-situ Dispersion of Core-shell Nanoparticle of Cu-Pt on In-situ Modified Carbon Surface and their Enhanced Electrocatalytic Activities

**Vishal M Dhavale, Sreekuttan M Unni, Husain N Kagalwala,
Vijayamohanan K Pillai, Sreekumar Kurungot**[*]

*Physical and Materials Chemistry Division, National Chemical Laboratory,
Pune-411008, India, Fax: +91-20-25902636; Tel: +91-20-25902566;*

E-mail: k.sreekumar@ncl.res.in

Experimental Section

1. Functionalization of Carbon:

All the chemicals required for the synthesis of the catalysts were procured from Sigma-Aldrich and used as such without any further purification. The functionalization of Vulcan-XC-72 (F-C) was done by giving an H_2O_2 treatment, employing a reported procedure. This mild oxidative treatment is an essential requirement as the active surface sites and functional groups generated during this process help interacting with the moieties formed from ascorbic acid (AA) during the course of the reduction process and self-oxidation.

2. Synthesis of Electrocatalyst:

Aqueous solution of $CuCl_2$ (0.1 N, 8 ml) was reduced by adding aqueous solution of AA (0.1 N, 40 ml). The mixture was stirred for 30 min. by maintaining the $_{P}$H at 12 by drop-wise addition of 10 % NaOH solution. At this stage copper gets reduced, as indicated by a reddish color, and instantaneously chloro-platinic acid solution (0.01 N, 8 ml) was added without altering the $_{P}$H of the mixture. The reaction mixture was kept under stirring for 20 min. at 60 ^{o}C to ensure complete reduction of Pt as indicated from the colour change of the mixture to black. F-C was dispersed in DI water by ultrasonication and instantly added in the reaction mixture and subsequently kept under stirring for 10 h. During this ageing time, the oxidation products of AA formed during the course of the metal ion reduction and degradation products of AA such as dehydroascorbic acid and 2, 3-diketogulonic acid help to modify the surface of carbon and anchor the core-shell nanoparticles. All the additions were done with a constant stirring of the reaction mixture. The catalyst (Cu@Pt/C) was filtered (filter paper 0.2 μm pore size, Rankem) and dried at 90 ^{o}C for 2 h. Since the core-shell particles are formed in the preceding step and subsequently anchored on the carbon surface in a sequential process, both excellent core-shell features and high dispersion could be simultaneously ensured in this process. Further to study the effect of shell thickness on the structure and properties of the core-shell materials, catalysts bearing different Pt weight percentage were synthesized (Table 1).

3. Structural Characterization:

The structure and morphology of these electrocatalysts were determined by a High Resolution Transmission Electron Microscope (HR-TEM). Sample for HR-TEM analysis was prepared by drop coating the sample (sonicated in isopropanol) on a carbon coated 200 mesh Cu grid and dried under vacuum and images were obtained on FEI, TECNAI G2 F30 instrument operated at an accelerated voltage of 300 kV (Cs = 0.6 mm, resolution 1.7 Å). X-ray diffraction patterns (XRD) patterns were recorded on PANalytical instrument using Cu-K_α radiation (λ =1.54 Å) at a scanning rate of 2 ^{o}min^{-1} and a step size of 0.02 ^{o} in 2θ. X-ray photoelectron spectroscopy (XPS) measurements were carried out on a VG Micro Tech ESCA 300^o instrument at a pressure of > 1 x 10^{-9} Torr (pass energy: 50 eV, electron take off angle: 60^o and the overall resolution: ~ 0.1 eV). Thermogravimetric experiments (TGA) were carried out in the temperature range of 0-1000 ^{o}C on a SDT Q600 TG-DTA analyzer under air atmosphere. Infra-Red (IR) Spectrum was recorded on PerkinElmer Instrument.

4. Electrochemical Studies:

Electrochemical properties were investigated by cyclic voltammetry (CV) and rotating disc electrode (RDE) studies using an Autolab PGSTAT30 (Eco-Chemie) instrument in a conventional three-electrode test cell with Hg/Hg_2SO_4 (MSE) as reference electrode (RE) and a platinum foil as a counter electrode (CE). Before preparation of the working electrode (WE), the catalyst slurry was made by sonicating 5 mg catalyst in 1 ml 3:2 ethanol-water mixture. The slurry was drop-coated on a previously polished (by using 0.3 μm alumina slurry) glassy carbon (GC) electrode surface (area = 0.071 cm^2) to achieve a loading of 4.5 μg-Pt. 2 μl of 0.01 wt % Nafion® solution was applied on the whole surface of the electrode to yield a uniform thin film. The electrode was dried for 2 h in air and used as the working electrode (WE) for electrochemical studies. An aqueous solution of 0.5 M H_2SO_4, de-aerated with N_2 gas, was used as an electrolyte for normal CV and RDE studies. Graphs were normalized by dividing current by geometrical area of electrode.

Results:

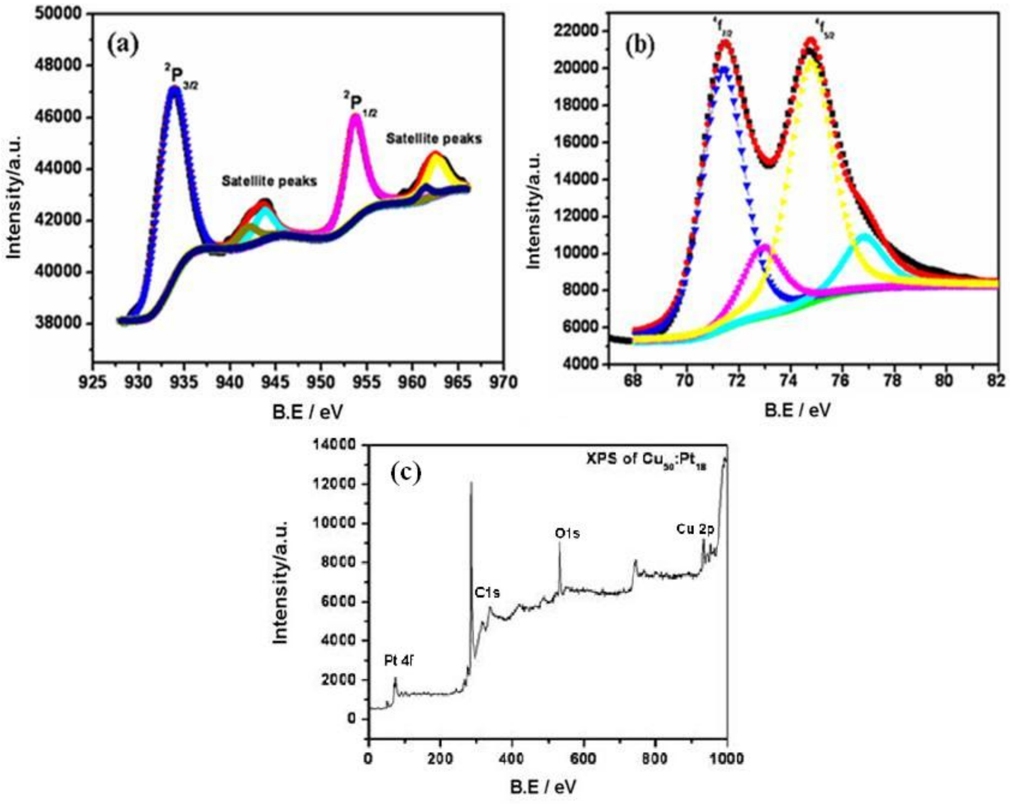

Fig. S1: *Deconvulated XPS spectra of (a) Cu, (b) Pt of* Cu_{50}:Pt_{18}, *Combined XPS spectra of* Cu_{50}:Pt_{18}.

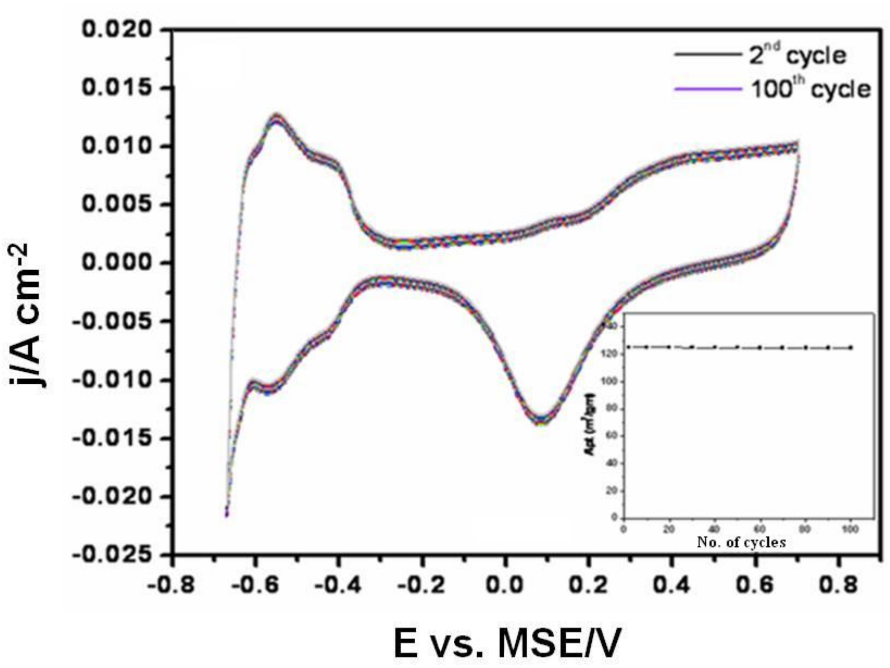

Fig. S2: *Durability study of* Cu_{50}*:*Pt_{18} *in 0.5 M* H_2SO_4 *electrolyte, performed at 100 mV* s^{-1} *for 100 cycles. The respective inset shows the graph of Apt versus number of cycles.*

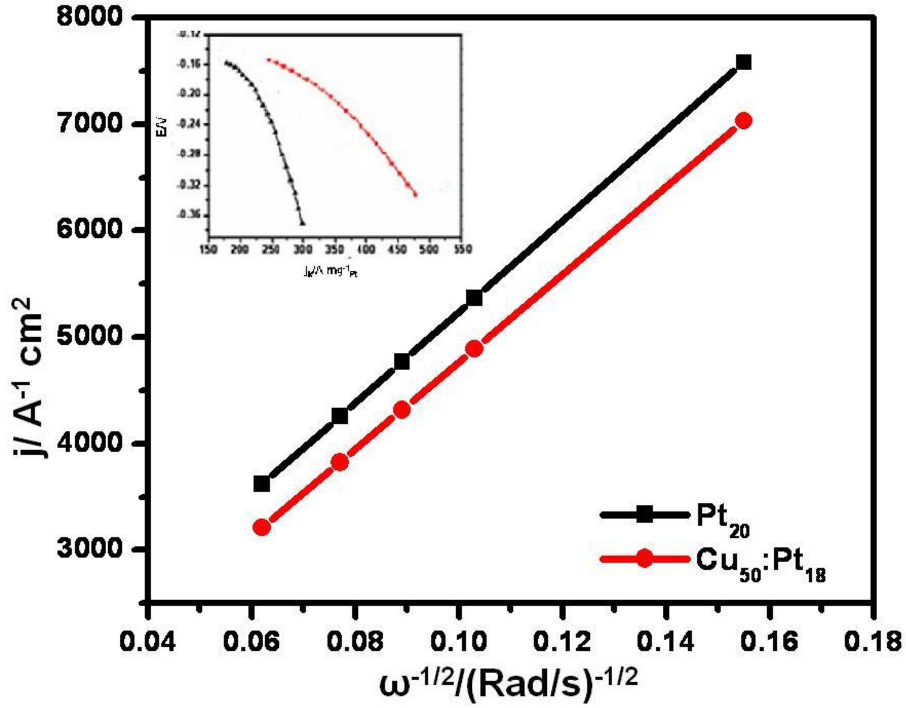

Fig. S3: *Koutecky–Levich (K-L) plots at -0.20 V and (inset) Tafel plots show core-shell catalyst have higher current density than that of* Pt_{20}. *Both were plotted from the RDE data.*

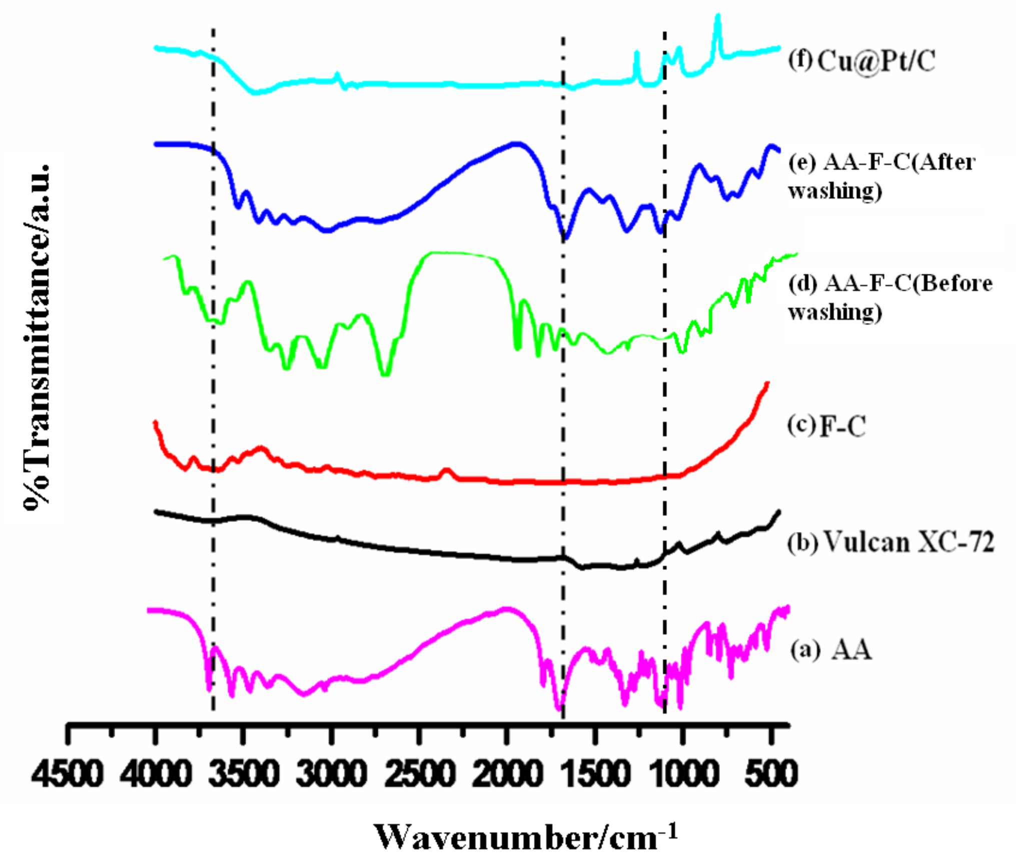

Fig. S4: *IR-spectra of (a) Ascorbic acid (AA), (b) Vulcan XC-72, (c) F-C, (d, e) AA treated F-C (AA-F-C) (before washing and after washing), (f) Cu@Pt/C.*

Fig. S4 shows the IR-Spectra of (a) ascorbic acid (AA), (b) Vulcan XC-72, (c) H_2-O_2 functionalized Vulcan XC-72 (F-C), (d, e) AA treated F-C (AA-F-C) before and after washing, respectively, and (f) after Cu_{50}:Pt_{18} nanoparticles dispersed on the AA-F-C. IR band at ~1740 cm^{-1} of the AA-F-C is attributed to the C=O stretching frequency of the dehydroascorbic acid and 2, 3-diketogulonic acid moieties formed during the reduction process. Moreover, the peaks in the finger print region due to the bending vibrations and the peaks at ~1050 cm^{-1} and ~1220 cm^{-1} due to the C-O stretching of acid and ether groups also give solid evidences of the new surface groups grafted on the surface. This clearly indicates that dispersion of Cu@Pt nanoparticles removes majority of the surface groups grafted on the surface. Also, since the core-shell particle decoration occurred in the medium consisting of AA and its degradation products, absence of the characteristic peaks of these moieties in the final product confirms that most of the residues could be removed by the washing step in the process work-up.

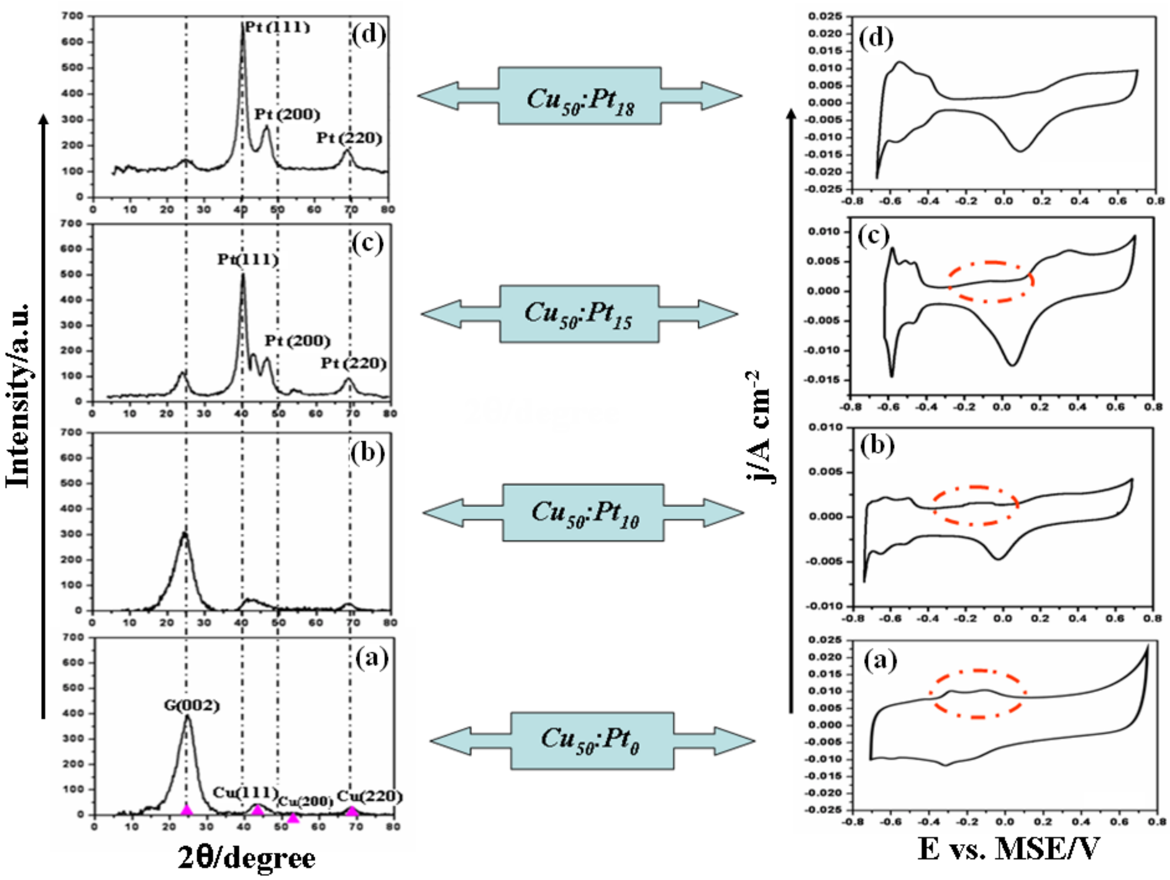

Fig. S5: *XRD spectrum (left) and cyclic voltammogram (right) of (a) Cu_{50}:Pt_0, (b) Cu_{50}:Pt_{10}, (c) Cu_{50}:Pt_{15}, (d) Cu_{50}:Pt_{18}.*

Fig. S5 (a, b, c, d) (left side) indicates the XRD patterns of the as synthesised catalysts with the different Cu:Pt compositions. The composition Cu_{50}:Pt_{18} shows diffraction patterns corresponding to the Pt (111), Pt (200), Pt (220) planes at 2θ = 39°, 46.5°, 68° without revealing any characteristic pattern of Cu planes. On the other hand, few characteristic Cu planes are visible along with the Pt planes in the other two Cu:Pt compositions, indicating incomplete coverage of the Cu surface by Pt layer in these two cases. This conclusion has been further supported by the cyclic voltammetric analysis (Fig. S5, right side) because the cyclicvoltammograms show the anodic peaks of Cu at -0.15 V (Vs. MSE) in the case of Cu_{50}:Pt_0, Cu_{50}:Pt_{10} and Cu_{50}:Pt_{15} (shown by the red colour circle), whereas this peak does not appear in the case of Cu_{50}:Pt_{18}. This result gives strong evidence on the formation of incessant Pt shell on the surface of the base metal when the Pt content increases to give the composition Cu_{50}:Pt_{18}.

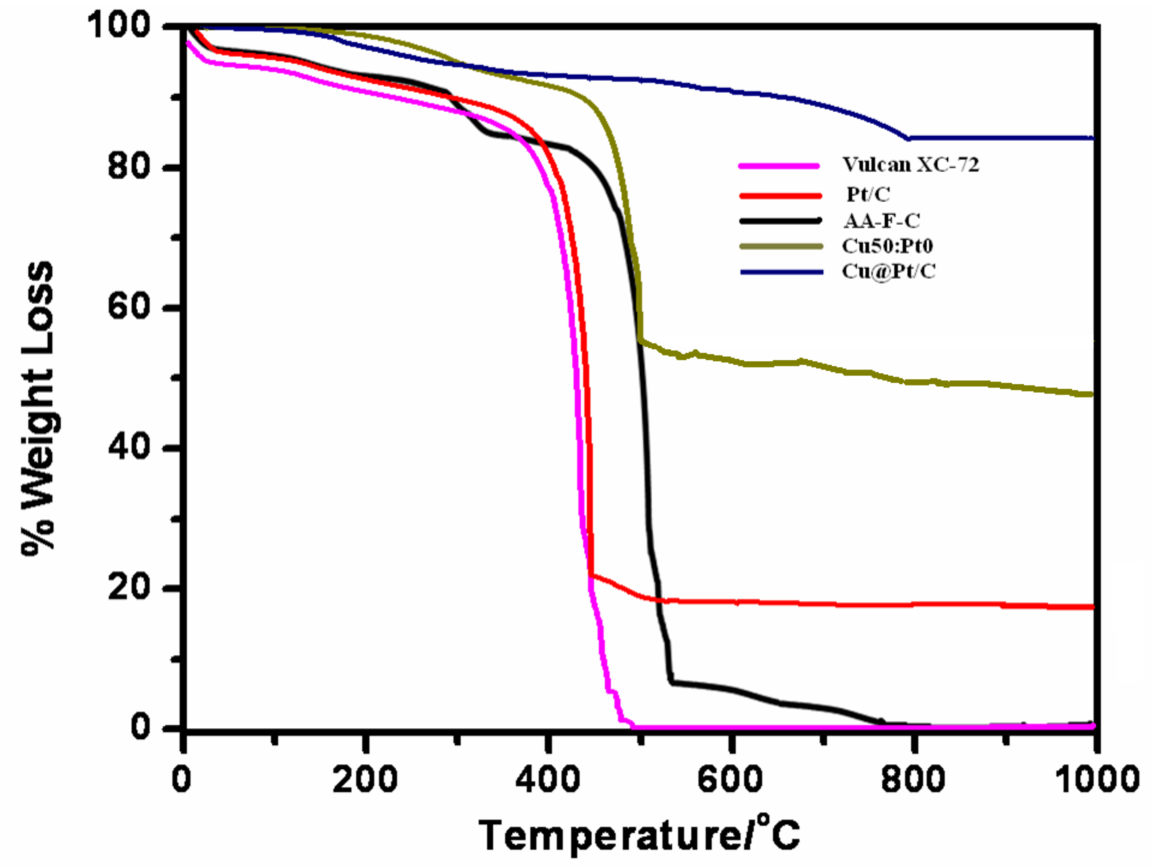

Fig. S6: *Thermo Gravimetric curve of Vulcan-XC-72, Pt/C (Pt_{20}), AA-F-C, Cu_{50}:Pt_0, Cu_{50}:Pt_{18}; performed in an air atmosphere.*

The thermal stability of the catalysts has been evaluated by Thermo Gravimetric Analysis (TGA) in an air atmosphere. TGA plots of Vulcan XC-72, Pt_{20} as well as the catalysts, namely Cu_{50}:Pt_0, AA treated F-C after washing (AA-F-C), and Cu_{50}:Pt_{18} (Fig. S 6) show an initial weight loss at 100 °C due to the loss of moisture. A prominent weight loss region has been observed in the case of AA-F-C in the proximity of 300 °C, which has been attributed to the loss of organic moieties adsorbed or deposited on the surface of carbon. The samples Cu_{50}:Pt_0 and Cu_{50}:Pt_{18} do not display prominent weight loss in this region, indicating nearly complete removal of the organic residues and moieties from the surface. Therefore, these results, along with the evidences from the IR and TEM analysis, rule out the possibilities of forming fibrous organic shells which can be originated during the decomposition of AA. Further loss in weight starting at 400 ^{o}C is attributed to the decomposition of carbon. Residual weight of 84 wt % in the case of Cu_{50}:Pt_{18} core-shell catalyst indicates the combined weight of Pt, Cu and the corresponding oxide forms of Cu.

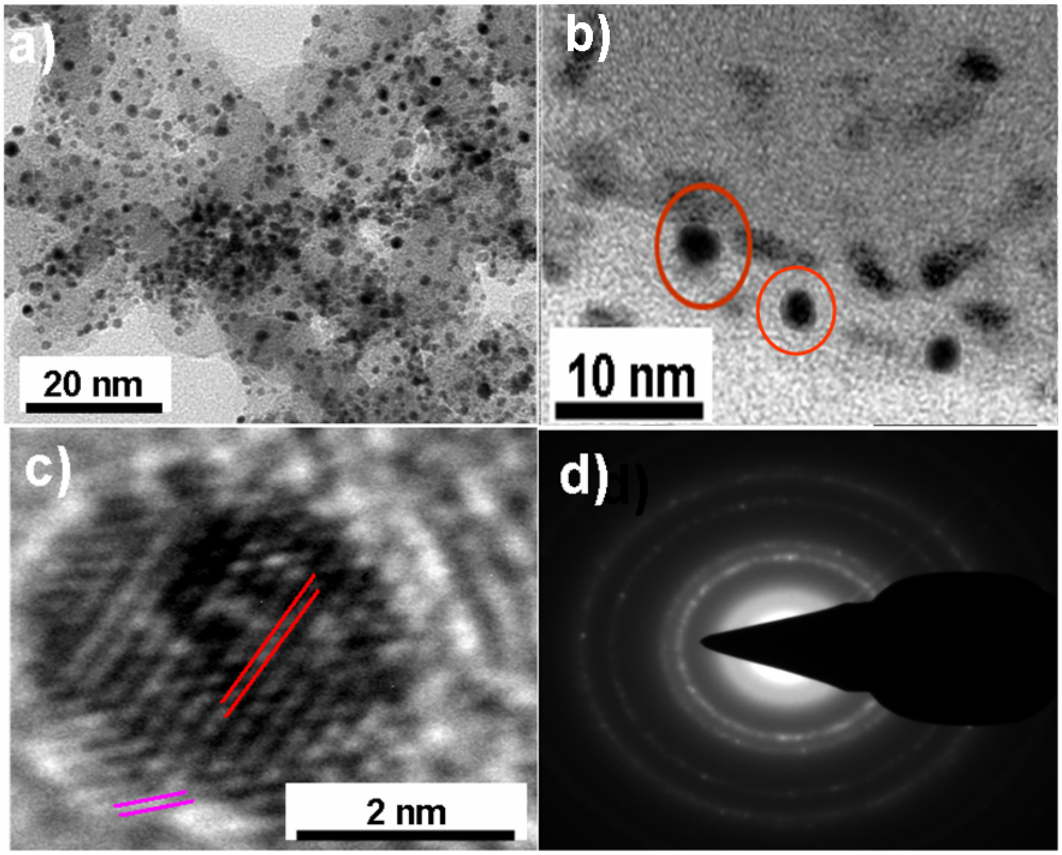

Fig. S7 *(a, b) TEM image of* Cu_{50}:Pt_{18} *at different resolution, (c) HR-TEM image of* Cu_{50}:Pt_{18} *with lattice fringes, (d) Selective area diffraction pattern (SADP).*

The TEM analysis provided images of Cu_{50}:Pt_{18} core-shell particles possessing thin shell of Pt on Cu. Since in a carbon supported core-shell catalyst, we have to simultaneously take care of the contrast differences of Cu, Pt and carbon, we faced some problems to simultaneously distinguish the contrast between Pt and carbon. However, better resolution could be obtained while focusing on the particles deposited along the curved edges (Fig. S7b) because focusing of such particles without the intervention of carbon was possible up to some extent. All those particles revealed essential features of the core-shell structure, possessing a thin Pt shell (~0.5 nm) on the non-noble metal core, giving an overall particle size of 3.0-4.0 nm. The difference between the interference fringes and their interpenetration at the interface of the two layers indicate the formation of crystalline core and shell structures, which can be seen in Fig. S7b. The calculated d-spacing values from selective area diffraction pattern (SAED) (Fig. S8d) are 3.37, 2.08 and 1.48 Å for Cu_{50}:Pt_{18}, which match with those of Pt (111), (200) and (220) planes.

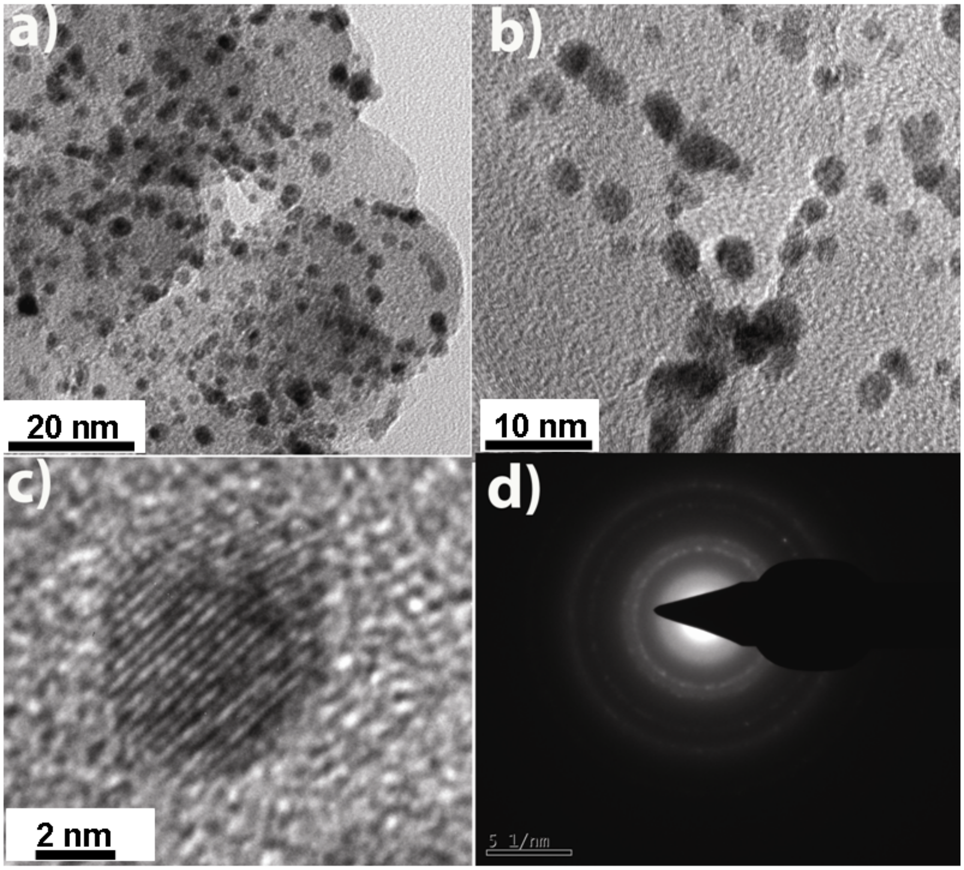

Fig. S8 *(a, b) TEM image of a commercial available Pt/C (Pt_{20}) at different resolution, (c) HR-TEM image of Pt_{20} with lattice fringes, (d) Selective area diffraction pattern (SADP) of Pt_{20}.*

We have also taken the TEM images of the commercially available Pt/C catalyst (Pt_{20}) which we have used as a standard sample for comparing the performance characteristics of the core-shell catalysts. As can be observed from Fig. S8a, the nanoparticles of Pt are well-dispersed with a mean particle size of ~ 3-5 nm. Moreover, most of the Pt particles have a spherical shape. Thus, both the P_{20} and core-shell catalysts have nearly similar dispersion and shape characteristics. The HR-TEM image Fig. S8c demonstrates good crystalline nature of the nanoparticles, matching with the Cu_{50}:Pt_{18} sample. The calculated d-spacing values from the SAED pattern are matching with (Fig. S8 d) with the (111), (200) and (220) planes of Pt.

Table 1: Synthesized catalyst with varying shell concentration

Cu@Pt/C				
Sr. No.	Sample Code Name	Cu: Pt: C ratio (Wt %)		
		Cu	Pt	C
1	Cu_{50}:Pt_{18}	50	18	32
2	Cu_{50}:Pt_{15}	50	15	35
3	Cu_{50}:Pt_{10}	50	10	40
4	Cu_{50}:Pt_{0}	50	0	50